

# 3D Hand Pose Estimation in Egocentric Images in the Wild

Aditya Prakash Ruisen Tu Matthew Chang Saurabh Gupta  
 University of Illinois Urbana-Champaign  
<https://bit.ly/WildHands>

## Abstract

We present *WildHands*, a method for 3D hand pose estimation in egocentric images in the wild. This is challenging due to (a) lack of 3D hand pose annotations for images in the wild, and (b) a form of perspective distortion-induced shape ambiguity that arises in the analysis of crops around hands. For the former, we use auxiliary supervision on in-the-wild data in the form of segmentation masks & grasp labels in addition to 3D supervision available in lab datasets. For the latter, we provide spatial cues about the location of the hand crop in the camera’s field of view. Our approach achieves the best 3D hand pose on the ARCTIC leaderboard and outperforms *FrankMocap*, a popular & robust approach for estimating hand pose in the wild, by 45.3% when evaluated on 2D hand pose on our EPIC-HandKps dataset.

## 1. Introduction

Understanding how hands interact with objects is crucial for applications in AR/VR [16, 24, 25], human-robot interaction [3, 32, 66], and robot learning [1, 6, 18, 47, 52, 55]. Towards this goal, 3D hand pose estimation is a vital step. Yet, no existing approach on this task performs satisfactorily on in-the-wild data. We focus on this gap and explore best practices in literature to design a system, *WildHands*, that works effectively on egocentric images in the wild (Fig. 1). *WildHands* outputs the 3D shape, 3D articulation and 3D placement of the hand in the camera coordinate frame.

This setting is quite challenging due to large perspective distortion (hands are close to the camera), poor visual signal (occlusion from the object of interaction, low resolution & motion blur) and lack of 3D pose annotations outside of controlled settings. We overcome these problems by using crops around hand (instead of full images [14]) while also encoding their location in the image, and using auxiliary supervision in the wild: segmentation [11] & grasp labels [8].

Let us unpack this a little. Common practice in predicting 3D hand pose [51, 61, 62], suggests using crops around the hand as input to the network. This exposes the model to fine-grained appearance information which could aid in



Figure 1. **WildHands** predicts the 3D shape, 3D articulation and 3D placement of the hand in the camera frame from a single in-the-wild egocentric RGB image & camera intrinsics. It produces better and more complete 3D output as compared to the popularly used *FrankMocap* [61], *e.g.* it captures the curl of the fingers more accurately as they interact with objects in challenging scenarios from EPIC-Kitchens [9] involving occlusion and dexterous interactions.

reasoning about the 3D pose. However, this increased resolution comes at a cost. Hands, as they move around in the camera’s field of view, undergo varying amounts of planar perspective distortion, as shown in Fig. 2. Working only with crops throws away information about the location of hand in the camera’s field of view and consequently the underlying perspective distortion. This loss of information leads to ambiguity (Sec. 3) in predicting the global pose of the hand (w.r.t. camera), on top of the inherent ambiguity in predicting 3D from a single image [56]. This ambiguity has also been identified in other settings in [54]. Following [54], we circumvent this perspective distortion induced shape ambiguity by providing information about the crop location to the model. This helps with the issue of large perspective distortion & poor visual signal.

However, it remains uncertain: How to get 3D hand pose estimation models to generalize to in-the-wild data for which it is hard to get 3D pose annotations? We tackle this issue by

using auxiliary supervision on in-the-wild data, specifically 2D hand masks [8, 11] & grasp labels [8], along with 3D pose supervision from in-the-lab datasets [14, 51]. Specifically, we use grasp labels predicted by the recently released model from [8] and use the ground truth segmentation masks available in VISOR [11]. To absorb supervision from segmentation labels, we differentially render [44] the predicted 3D hand into images and back-propagate the loss through the rendering. For grasp supervision, we note that hand pose is indicative of the grasp type and use supervision from a grasp classifier that takes the predicted 3D hand pose as input.

While several datasets [14, 16, 22, 23, 43] contain 3D ground truth for evaluating 3D poses, they are collected in controlled setups which may not represent the challenges of in-the-wild [11, 19] settings. These annotations are typically collected with marker-based MoCap setup [14, 70] or multi-view reconstruction from a multi-camera setup [7, 22, 51]. In the absence of these setups, collecting 3D ground truth for hand poses in the wild is quite difficult. Instead, it is feasible to collect annotations for 2D hand keypoints in the image and use them to evaluate *the 2D projections of the predicted 3D hand pose*. To enable this, we collect 2D hand joint annotations on 5K images from in-the-wild EPIC-Kitchens VISOR [11] dataset and use it for evaluating different models. We refer to this dataset as EPIC-HandKps.

We directly evaluate the quality of our 3D output on two recent egocentric datasets with 3D ground truth: ARCTIC [14] & AssemblyHands [51]. We conduct an indirect evaluation on in-the-wild data by measuring error in 2D projections of our 3D output on our collected EPIC-HandKps dataset. WildHands achieves the best hand pose score on the online ARCTIC leaderboard [14] (as of Nov 17, 2023) in the egocentric setting. In our experiments (Sec. 5), we outperform recent approach from Fan *et al.* [14] by 10.8% on ARCTIC and 17.6% on AssemblyHands. On EPIC-HandKps, we obtain 45.3% relative improvement over FrankMocap [61], a robust and popular hand pose estimation approach.

**Contributions:** (1) We present WildHands, a system for 3D hand pose estimation from egocentric images in the wild. (2) We collect EPIC-HandKps, containing 2D hand keypoint annotations on 5K images from in-the-wild EPIC-Kitchens VISOR dataset to evaluate 2D projects of estimated 3D hand pose. (3) WildHands achieves the best 3D hand pose scores on the ARCTIC egocentric leaderboard and improves by 45.3% over FrankMocap on the EPIC-HandKps dataset.

## 2. Related Work

**Hand pose estimation & reconstruction:** Several decades of work [15, 30, 58] have studied different aspects: 2D pose [7, 65] vs. 3D pose [41, 51, 71, 74] vs. mesh [2, 27, 67], RGB [14, 23, 27] vs. RGBD [59, 64, 65, 68, 69, 71] inputs, egocentric [14, 51] vs. allocentric [14, 22, 23], hands in



Figure 2. Perspective distortion in planar projection as the same hand moves across the camera’s field of view from left to right.

isolation [50, 80] vs. interaction with objects [22, 46, 75], feed-forward prediction [14, 23, 27, 62] vs. test-time optimization [5, 28]. Driven by the advances in parametric hand models [53, 60], recent work has moved past 3D joint estimation towards 3D mesh recovery [14, 23, 27, 61, 78]. Papers have tackled these problems in 3 contexts: single hands in isolation [79], hands interacting with objects [14, 73] & two hands interacting with one another [23, 50]. Jointly reasoning about hands & objects has proved fruitful to improve both hand & object reconstruction [27, 38, 76]. While several expressive models focus on 3D hand pose estimation [23, 33–35, 62], they do not consider egocentric datasets in the wild. We focus on this setting due to challenges involving dynamic interactions & heavy occlusions. The most related to our work is [14] which predicts 3D hand pose, represented using MANO [60] in egocentric settings involving dexterous hand-object interactions. We build on their ArcticNet-SF [14] model by including hand crops [61], crop location information & auxiliary supervision from in-the-wild datasets to design a system that works well in the wild.

**Hand datasets:** Since 3D hand pose annotations from single images is difficult, most datasets are collected in controlled settings to get 3D ground truth using MoCap [14, 70], multi-camera setups [22, 23, 41, 46, 51], or magnetic sensors [17]. They often include single hands in isolation [80], hand-object interactions [14, 22, 23, 41] & hand-hand interactions [50]. Different from these datasets with 3D poses, [8, 11, 63] provide annotations for segmentation masks [8, 11], 2D bounding boxes [63] and grasp labels [8] on internet videos [63] and egocentric images in the wild [9, 19]. Our work combines 3D supervision from datasets [14, 51] captured in controlled settings with 2D auxiliary supervision, *i.e.* segmentation masks & grasp labels, from in-the-wild datasets [8, 11] to learn models that perform well in the wild. We also collect EPIC-HandKps dataset with 2D hand keypoints on 5K images from EPIC-Kitchens for in-the-wild evaluation.

**Auxiliary supervision:** Several works on 3D shape prediction from a single image [36, 72] often use auxiliary supervision to deal with lack of 3D annotations. [36] uses keypoint supervision for 3D human mesh recovery, while [72] uses multi-view consistency cues for 3D object reconstruction. Aided by differentiable rendering [39, 45], segmentation and depth prediction have also been used to provide supervision for 3D reconstruction [5, 28, 37]. We adopt this use of segmentation as an auxiliary cue for 3D poses. In addition, we

also use supervision from hand grasp labels based on the insight that hand grasp is indicative of the hand pose.

**Ambiguity:** 3D estimation from a single image is ill-posed due to ambiguities arising from scale-depth confusion [26] and cropping [54]. Recent work [54] points out the presence of perspective distortion-induced shape ambiguity in image crops and uses camera intrinsic-based location encodings to mitigate it. We investigate the presence of this ambiguity for hand crops in egocentric images and adopt the proposed embedding to mitigate it. Similar embeddings have been used before in literature, primarily from the point of view of training models on images from different cameras [12, 21], to encode extrinsic information [20, 49, 77].

### 3. 3D Hand Pose Ambiguity in Image Crops due to Perspective Distortion

Depending on the location in the camera’s field of view, the same object looks different due to perspective distortion, as shown in Fig. 2. Prakash *et al.* [54] note that this distortion creates ambiguity in perceiving shape from image crops, *i.e.* the same crop could correspond to different underlying 3D shapes depending on its location. Note that 3D from a single image is already an under-constrained task. Working with image crops, without keeping track of where the crop came from, further exaggerates this ambiguity. In this section, we verify if using crops around hands in egocentric images also lead to a similar additional shape ambiguity.

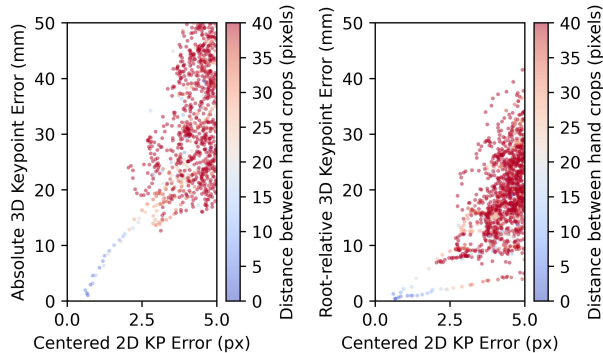
To answer this question, we analyze right hands in the ARCTIC [14] dataset since it contains 3D annotations for hand joints at different locations in the image. Consider the following distances between a pair of hands:

- **Pixel distance between hand crops**, measured as the pixel distance between the centroid of the 2D hand keypoints from the two hands.
- **Centered 2D keypoint error**, measures the average pairwise pixel distance between 2D keypoints from the 2 hands, *after bringing their centroids to the origin*.
- **Absolute 3D keypoint error**, as the residual between 3D keypoints to measure 3D shape mismatch between hands,
- **Root relative 3D keypoint error**, as the residual between the 3D keypoints *after aligning the root joints in location and orientation*.

Fig. 3 (a.1) and Fig. 3 (a.2) plots these distances between a reference hand and all other hands in ARCTIC. X-axis plots the centered 2D keypoint error (in pixels), Y-axis plots the 3D keypoint error between hands (absolute in a.1 and root-relative in a.2, in mm). The color of the point denotes the pixel distance between the hand crops.

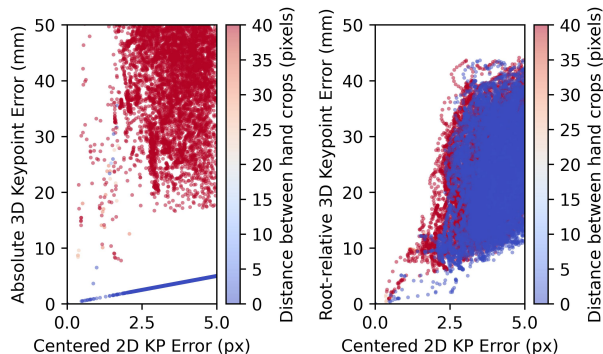
When constraining the crop to be around the reference hand location (blue points in the plots) the 3D error is small, *i.e.* there is only a small amount of ambiguity. However, when we let the crop be anywhere in the image (the red

(a) 3D hands as they occur in ARCTIC



(a.1) Absolute 3D Error (a.2) Root relative 3D Error

(b) 3D hands from ARCTIC after alignment to crop



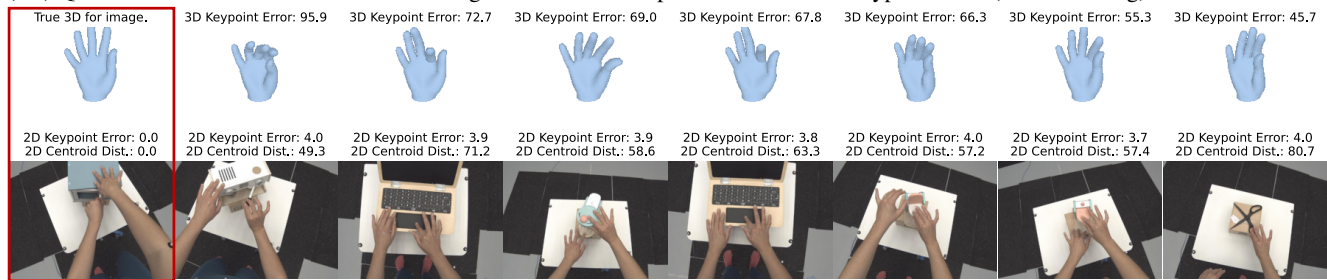
(b.1) Absolute 3D Error (b.2) Root relative 3D Error

Figure 3. **3D Hand Pose Ambiguity in Image Crops due to Perspective Distortion.** (a) We plot 3D keypoint error in hands (absolute in (a.1) and root relative in (a.2)) vs. centered 2D keypoint error in hand crops for the hands in the ARCTIC dataset against a reference hand. Color of the points indicates the distance between hand crops (blue is near, red is far). *The red points denote the additional ambiguity induced by ignoring the 2D location of the hand crop in the visual field over and above the ambiguity of making 3D inferences from 2D images depicted by the blue points.* (b) shows similar plots but after aligning hands in ARCTIC to the reference crop with and without shifts to account for the varying density in the distribution of hands across the image.

points), even though the 2D keypoints within the crop are very similar, the 3D hand pose is quite different. The additional height of the red points denotes the *additional* ambiguity induced by ignoring the 2D location of the hand crop in the visual field on top of the ambiguity of making 3D inferences from 2D images (depicted by the blue points). Both absolute and root-relative 3D shape exhibit ambiguity. Fig. 4 (a.1 and a.2) show examples of hands that have high 3D shape error but low centered 2D keypoint error.

One may question if the additional ambiguity arises due to larger number of crops present at arbitrary locations in

(a.1) Qualitative visualizations for hands with high **absolute** 3D shape error but low 2D keypoint error (after centering).



(a.2) Qualitative visualizations for hands with high **root-relative** 3D shape error but low 2D keypoint error (after centering).

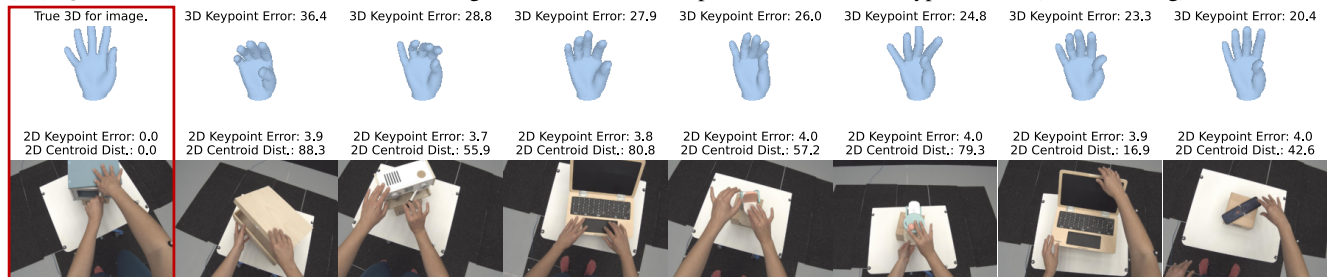


Figure 4. **Ambiguity in Absolute and Root-Relative Hand Shape.** We visualize hands with high 3D shape error (absolute in (a.1) and root-relative in (a.2)) but low 2D keypoint error (after centering). The right hand in the 1<sup>st</sup> frame is the reference hand w.r.t. which we measure 2D and 3D keypoint errors. We observe a large deviation in 3D shape (*i.e.* large 3D keypoint w.r.t. reference hand) as we let the hand crop move around in the camera’s field of view, even though 2D keypoint error is low.

the image compared to crops that are close to the reference hand. Fig. 3 (bottom row) conducts the same analysis but after a PnP alignment [42] between the 2D keypoints for the reference hand and all 3D hands in ARCTIC. We do one alignment the default way, where PnP searches for the 3D rotation and translation that best aligns a hand to the 2D keypoints of the reference hand. We do another alignment that additionally allows for an arbitrary 2D shift in the hand keypoints for the reference hands. We compute the same distances for each aligned 3D hand in the dataset and plot them together in Fig. 3 (b.1) and Fig. 3 (b.2). Note the additional ambiguity for when shifts are allowed (red points) vs. when they are not (blue points). Figure in Supp. shows qualitative examples for the hand shape and the corresponding location in the field of view after the PnP alignment to the reference 2D keypoints with appropriate shifts.

## 4. Method

We present a novel approach, WildHands, for 3D hand pose estimation from egocentric images in the wild. We build on top of ArcticNet-SF [14] and FrankMocap [61]. Given a crop around a hand and associated camera intrinsics, WildHands predicts the 3D hand shape, its articulation, and global pose w.r.t. the camera. We adopt MANO [60] to represent the 3D hand, parameterized by shape  $\beta$  and angles of articulation  $\theta_{\text{local}}$  for 15 hand joints. WildHands uses a neural network to

predict  $\beta$ ,  $\theta_{\text{local}}$  and the global pose  $\theta_{\text{global}}$  of the root joint.

Fig. 5 provides an overview of our model. Our network operates on crops around hands. We use a ResNet50 [29] backbone pretrained on ImageNet to obtain a  $7 \times 7 \times 2048$  feature representation for the hand crop. We process this feature map through 3 convolutional and 2 linear layers to map into a 2048-dimensional feature vector. This is passed to a HMR [37] decoder to predict the hand parameters: shape  $\beta$ , articulation  $\theta_{\text{local}}$ , and global pose  $\theta_{\text{global}}$ .

Our contribution lies in the use of (1) intrinsics-aware positional encoding (KPE [54]) to input information about the position of the hand crop in the visual field, and (2) auxiliary sources of supervision to train the model on in-the-wild data where 3D ground truth is not available.

### 4.1. Using Hand Crop Location To Mitigate Perspective Distortion-induced Shape Ambiguity

We use KPE [54] to mitigate the perspective distortion-induced shape ambiguity discussed in Sec. 3. Specifically, we provide the network with information about the location of the hand crop in camera’s visual field. Let us denote the camera’s principal point as  $(p_x, p_y)$  and focal length as  $(f_x, f_y)$ . For each pixel  $(x, y)$ , we first compute the angles,  $\theta_x = \tan^{-1}\left(\frac{x-p_x}{f_x}\right)$  and  $\theta_y = \tan^{-1}\left(\frac{y-p_y}{f_y}\right)$ , convert it into a sinusoidal encoding [48] with 4 frequency components and concatenate with the features from the convolutional

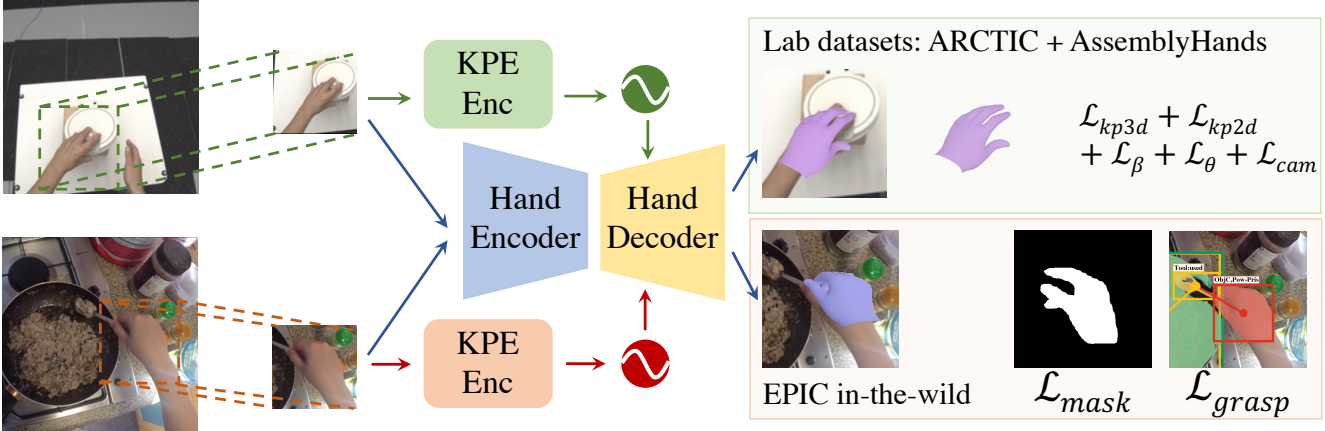


Figure 5. **Model Overview.** We crop the input images around the hand and process them using a convolutional backbone. The hand features along with the global image features (not shown above for clarity) and intrinsics-aware positional encoding (KPE [54]) for each crop are fed to the decoder to predict the 3D hand. The hand decoders predict MANO parameters  $\beta$ ,  $\theta_{local}$ ,  $\theta_{global}$  and camera translation which are converted to 3D keypoints & 2D keypoints and trained using 3D supervision on lab datasets, e.g. ARCTIC [14], AssemblyHands [51]. We also use auxiliary supervision from in-the-wild EPIC-Kitchens [11] dataset via hand segmentation masks and grasp labels. The hand masks are available with the VISOR dataset [11] whereas grasp labels are estimated using off-the-shelf model from [8].

backbones. We consider two design choices: encoding the center and corners of the cropped box and using a dense spatial encoding for all pixels in the crop. The crop’s position allows the network to adapt its interpretation to the different parts of the visual field as appropriate.

## 4.2. Auxiliary Supervision on In-the-wild Data

While 3D supervision can be used to train models on datasets collected in controlled settings, such annotations are hard to collect in the wild. This drastically limits the diversity of data that the model is trained on, thereby limiting their applicability to in-the-wild settings. To circumvent this issue, we use auxiliary 2D supervision in the form of hand segmentation masks and grasp labels on egocentric images from in-the-wild EPIC-Kitchens [10] dataset.

**Supervision from Segmentation Masks:** Our model outputs  $\beta$ ,  $\theta_{local}$ , and  $\theta_{global}$  for the predicted hand, which is passed to a differentiable MANO layer [27, 60] to get the hand vertices. These vertices are used to differentially render a soft segmentation mask using SoftRasterizer [45, 57]. We supervise the rendered soft segmentation mask to match the ground truth segmentation mask using L1 loss, following [5, 28]. We use the ground truth segmentations from VISOR [11] and only apply this loss on amodal masks (*i.e.* hand masks that are known to not be interrupted by objects).

**Supervision from Grasp Labels:** We use the insight that grasp type during interaction with objects is indicative of hand pose. We train a grasp prediction head on  $\theta_{local}$  predicted by WildHands via a 4-layer MLP. This MLP predicts logits for the 8 different grasp classes defined in [8]. The MLP and the WildHands model are jointly trained using a

cross-entropy loss against ground truth grasp labels, computed using an off-the-shelf model from [8].

## 4.3. Implementation Details

We train WildHands jointly on multiple datasets: (1) ARCTIC [14]: using 3D supervision on  $\beta$ ,  $\theta_{local}$ ,  $\theta_{global}$ , 3D hand keypoints and 2D projections of 3D keypoints in the image, (2) AssemblyHands [51]: using supervision on 3D hand keypoints and 2D projections of 3D keypoints in the image (it does not represent hands using MANO), and (3) EPIC-Kitchens [10]: using segmentation masks and grasp labels. Following [14], we use L2 loss for  $\beta$ ,  $\theta_{local}$ ,  $\theta_{global}$ , 3D keypoints and 2D keypoints. L1 loss is used for segmentation masks and cross-entropy loss for grasp labels. We use the official splits for training and validation on each dataset. We initialize our model with the ArcticNet-SF model trained on the allocentric split of the ARCTIC dataset [14]. All models are trained for 100 epochs with a learning rate of  $1e-5$ . More details are provided in the supplementary.

## 5. Experiments

We conduct experiments in 2 settings: 3D hand pose evaluation on ARCTIC [14] & AssemblyHands [51] and 2D hand keypoint evaluation on our EPIC-HandKps dataset. The experiments are geared towards analyzing the effectiveness of our architectural design choices (using crops, KPE encoding), different terms in the loss function, impact of different datasets used for training in both 3D and 2D pose evaluation.

**Datasets:** We use ARCTIC [14] and AssemblyHands [51] for 3D pose evaluation. We select ARCTIC since it contains the largest range of hand pose variation [14] among existing

Method	3D pose on ARCTIC val		2D pose on EPIC-HandKps		
	MPJPE	MRRPE	Right hand	Left hand	Aggregate
FrankMocap [61]	53.99	no global pose	13.02	13.74	13.33
ArcticNet-SF [14]	22.60	32.71	33.67	36.94	35.07
HandNet	21.50	58.13	32.24	30.79	31.62
WildHands	<b>20.57</b>	<b>28.81</b>	<b>6.51</b>	<b>6.90</b>	<b>6.68</b>

Table 1. **WildHands outperforms state-of-the-art in direct 3D evaluation on ARCTIC [14] and indirect 2D evaluation on in-the-wild data from EPIC-HandKps.**

Method	MPJPE	MRRPE
ArcticNet-SF	19.18	28.31
ArcticOccNet	19.77	29.75
DIGIT-HRNet	16.74	25.49
HMR-ResNet50	20.32	32.32
RWTH-CVG	16.33	26.07
WildHands	<b>15.72</b>	<b>23.88</b>

Table 2. **WildHands leads the 3D hand pose ARCTIC leaderboard as of Nov 17, 2023.**

datasets [7, 22, 23, 46, 70]. It contains 393 sequences of dexterous manipulation of 11 articulated objects by 10 subjects from 8 static views & 1 egocentric view, paired with 3D hand & object meshes. We focus on the egocentric setting which contains 200K images and use the official splits: 187K train, 20k val and 25k test images. The ground truth for the test set is not publicly available and the evaluation is done on a public leaderboard. We also consider AssemblyHands since it is a large-scale dataset with more than 360K egocentric images in the train split.

We use egocentric images from EPIC-Kitchens as in-the-wild data for training our model using auxiliary supervision. We use 30K images for training available in the VISOR split of EPIC-Kitchens. We obtain modal/amodal labels for these images and train using segmentation mask supervision only on the images with amodal mask. For obtaining grasp labels on these images, we use off-the-shelf model from [8] which outputs 8-way grasp classification. For evaluation, we collect 2D hand keypoints annotations on 5K egocentric images from validation split of VISOR.

**Metrics:** For 3D hand pose evaluation, we adopt the protocol from ARCTIC. We consider 2 metrics: (1) Mean Per-Joint Position Error (MPJPE): L2 distance (mm) between the 21 predicted and ground truth joints for each hand after subtracting the root joint, (2) Mean Relative-Root Position Error (MRRPE): the translation between the root joints of left hand and right hand, following [13, 14, 50]. For evaluation on in-the-wild data, we measure the L2 distance (in pixels) between ground truth 2D hand keypoints and 2D re-projections of 3D keypoints output from our model.

**Baselines:** (1) ArcticNet-SF [14] is the single-image model released with the ARCTIC benchmark. It consists of a convolutional backbone (ResNet50 [29]) to process the input image, followed by a HMR [37]-style decoder to predict the hand and object poses. We focus on the hands, which are represented using MANO [60] parameterization. (2) FrankMocap [61] is trained on multiple datasets collected in controlled settings, which makes it the most robust to apply in in-the-wild setting [5, 28, 76]. It uses hand crops as input instead of the entire image, which is then processed by a con-

volutional backbone. The decoder is similar to HMR [37] which outputs MANO parameters for hand and training is done using 3D pose & 2D keypoints supervision. (3) HandNet: Since the training code is not available for FrankMocap, we are unable to train it in our setting. So, we implement a version of ArcticNet-SF which uses crops as input along with HMR-style decoder and train it in our setting using 3D & 2D hand ground truth available on ARCTIC & AssemblyHands. (4) ARCTIC has a public leaderboard consisting of several models with convolutional (*e.g.* ArcticNet-SF, DIGIT-HRNet, HMR-ResNet50) and transformer architectures (*e.g.* RWTH-CVG). Most of these models are not publicly available, so it is not possible to do a detailed comparison.

## 5.1. Results

We now present our key results. We compare WildHands with relevant baselines on the EPIC-HandKps datasets (Tab. 1), ARCTIC (Tab. 1) & AssemblyHands validation sets (Tab. 3) and the ARCTIC leaderboard (Tab. 2).

**Evaluation in the wild:** Since our focus is on in-the-wild settings, we first discuss the 2D hand pose results on VISOR. We compare with ArcticNet-SF, HandNet & FrankMocap, which is the most robust approach in the wild. From the results in Tab. 1, our method outperforms FrankMocap by 45.3%. Moreover, models trained with 3D & 2D hand annotations on lab datasets do not generalize well to EPIC-HandKps. This is likely due to the domain gap between the lab datasets and in-the-wild settings.

**3D hand poses on ARCTIC:** The goal of this experiment is to see if the gains in 2D pose transfer to 3D pose as well. In Tab. 1, the performance of FrankMocap degrades considerably in ARCTIC setting. This is expected since FrankMocap is not trained on egocentric datasets. Next, we observe that ArcticNet-SF (trained on ARCTIC) does better than FrankMocap on ARCTIC evaluation, but performs worse on EPIC-HandKps. We notice a similar trend for HandNet which is trained with hand crops as input on both ARCTIC & AssemblyHands. Compared to these baselines, our full model performs the best across all 3D & 2D metrics.

Method	network input	KPE encoding	Assembly val	
			MPJPE	MRRPE
ArcticNet-SF	image	n/a	23.96	58.21
WildHands (no aux.)	crop	n/a	22.55	53.92
WildHands (no aux.)	crop	sparse	22.24	35.58
above model + ARCTIC	crop	sparse	<b>19.72</b>	<b>28.13</b>

Table 3. **Results on AssemblyHands.** Using crops and KPE encodings also improve performance when training and testing on the AssmeblyHands dataset.

Method	network input	KPE encoding	ARCTIC val		EPIC-HandKps
			MPJPE	MRRPE	L2 error
ArcticNet-SF [14]	image	n/a	22.60	32.71	35.07
WildHands (no aux.)	crop	-	21.40	58.24	34.12
WildHands (no aux.)	crop	dense	<b>21.13</b>	<b>30.20</b>	19.99
WildHands (no aux.)	crop	sparse	21.50	<b>28.70</b>	<b>17.07</b>
<i>WildHands (full)</i>	<i>crop</i>	<i>sparse</i>	<i>20.57</i>	<i>28.81</i>	<i>6.68</i>

Table 4. **Role of Cropping and KPE Encoding.** Switching to crops from full image input (as used in ArcticNet-SF [14]), we see a small improvement in root relative shape metric (MPJPE) but a huge degradation in global pose metrics (MRRPE). Adding in the KPE encoding, either sparse or dense, maintains the root relative shape metric, but improves the global pose metric significantly, while also improving the EPIC-HandKps metrics. To maximally isolate the impact of cropping and KPE encodings, these comparisons are done without any auxiliary supervision. As a reference, we also present the performance of our full system that also uses the auxiliary supervision on in-the-wild data in the last row.

**Leaderboard evaluation:** On the public ARCTIC leaderboard, our method achieves the best hand pose results compared to other submissions. These submissions consist of both convolutional (*e.g.* ArcticNet-SF, DIGIT-HRNet, HMR-ResNet50) and transformer models (*e.g.* RWTH-CVG).

**3D Evaluation on AssemblyHands:** From the results in Tab. 3, we observe a similar trend as before, with our model achieving the best 3D and 2D hand pose scores. Note that our evaluation setting is different than the AssemblyHands leaderboard since we do not consider access to ground truth depth of the root joint. This is because this privilege information is not available in in-the-wild settings.

## 5.2. Ablation Study

Next, we conduct ablation study to show the effectiveness of different components in our method: use of crops and KPE encoding (Tab. 4), different loss terms (Tab. 5), and datasets used for training (Tab. 6).

**Role of cropping and KPE:** From the results in Tab. 4, we observe that using crops as input instead of the full image improves the MPJPE and 2D poses but MRRPE score gets worse. This is expected since the model gets to focus better on each hand but also loses information about the spatial

Method	ARCTIC val		EPIC-HandKps
	MPJPE ↓	MRRPE ↓	L2 error ↓
WildHands	<b>20.57</b>	28.81	<b>6.68</b>
– grasp	21.64	30.52	9.27
– segmentation	20.99	29.75	13.60
– grasp – segmentation	21.50	<b>28.70</b>	17.07

Table 5. **Role of auxiliary supervision.** Both grasp and segmentation auxiliary supervision contribute to the final performance, with segmentation providing a bigger gain as compared to grasp labels.

Training Datasets	ARCTIC val		EPIC-HandKps
	MPJPE	MRRPE	L2 error
ARCTIC	21.50	<b>28.70</b>	17.07
ARCTIC + Assembly	23.20	30.00	11.05
ARCTIC + VISOR (aux)	<b>20.57</b>	28.81	6.68
ARCTIC + Assembly + VISOR (aux)	21.76	29.66	<b>6.56</b>

Table 6. **Effect of Scaling-up Data.** While additional datasets on top of the ARCTIC data don’t improve metrics on ARCTIC, adding either Assembly (3D supervision) or VISOR (with auxiliary supervision) improves metrics on EPIC-HandKps, with the auxiliary supervision from the in domain VISOR data helping more.

location of the hand. Next, we observe that using the KPE helps mitigate this issue and greatly improves the MRRPE and 2D pose errors. We explore both the dense and sparse variants of KPE and find the sparse variant to work better.

**Role of auxiliary supervision:** We ablate the different auxiliary sources of supervision used in our model and their design choices in Tab. 5. We add this supervision on top of the model trained on ARCTIC. We observe that using grasp labels improves MPJPE & 2D pose and slightly deteriorates the MRRPE scores. We try 2 variants of the grasp labels supervision: with the global image features and without. The variant without the global features performs better on EPIC-HandKps, indicating that the network needs to rely on a better hand pose in the absence of global features. Next, we observe that deriving supervision from hand masks using differentiable rendering is highly effective and contributes to the most gain in performance. Finally, combining both segmentation masks and grasp supervision leads to further improvement in both 3D and 2D poses.

**Role of different datasets:** Since our model is trained on ARCTIC, AssemblyHands and EPIC-Kitchens, it is important to understand the benefits due to each. We show these results in Tab. 6. We notice that training on both ARCTIC and AssemblyHands leads to better 2D pose on EPIC-HandKps, even outperforming FrankMocap in zero-shot setting. However, the 3D pose on ARCTIC gets worse. This could be due to domain gap between ARCTIC and AssemblyHands since AssemblyHands only has grayscale images in the egocentric setting. This is also evi-

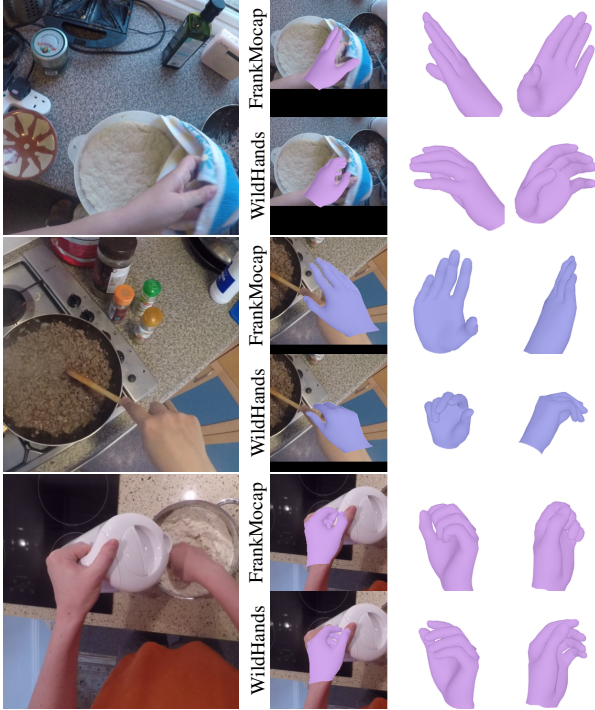


Figure 6. **Visualizations on EPIC-HandKps.** Our WildHands model is able to predict better hand poses from a single image than FrankMocap [61] in challenging occlusion scenarios involving dexterous interactions, *e.g.* images of hands grasping the objects from EPIC-HandKps. We show projection of the predicted hand in the image and rendering of the hand mesh from 2 more views.

dent from comparing ARCTIC+VISOR model with ARCTIC+AssemblyHands+VISOR model where the latter performs worse on ARCTIC even though doing slightly better on EPIC-HandKps. This indicates that auxiliary supervision from VISOR is quite effective in egocentric settings on both ARCTIC and EPIC-HandKps.

### 5.3. Visualizations

We show qualitative comparisons of the hand pose, predicted by WildHands, with FrankMocap on EPIC-HandKps (Fig. 6) and ArcticNet-SF on ARCTIC (Fig. 7). Looking at the projection of the mesh in the camera view and rendering of the mesh from additional views, we observe that WildHands is able to predict hand pose better in images involving occlusion and interaction, *e.g.* fingers are curled around the object in contact (Fig. 6) for our model but this is not the case for FrankMocap. We observe similar trends in ARCTIC (Fig. 7) as well where our model predicts better hands in contact scenarios. More visualizations are in supplementary.

**Limitations:** The KPE encoding used in our model requires camera intrinsics to be known, which may not be available in certain scenarios. However, in several in-the-wild images, the metadata often contains camera information. Also, we currently set the weights for different loss terms as hy-

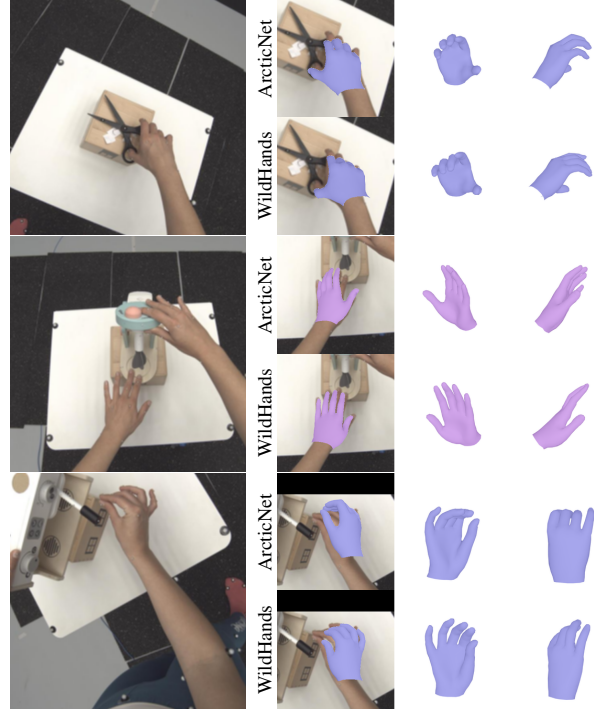


Figure 7. **Visualizations on ARCTIC.** Our WildHands model is able to predict better hand poses from a single image than ArcticNet-SF [61] in scenes involving interaction with articulated objects. We show projection of the predicted hand in the image and rendering of the hand mesh from 2 additional views.

perparameters which may not be ideal since the sources of supervision are quite different leading to different scales in loss values. It could be useful to use a learned weighing scheme, *e.g.* uncertainty-based loss weighting [4, 31, 40].

## 6. Conclusion

We present WildHands, a system that adapts best practices from the literature: using crops as input, intrinsics-aware positional encoding, auxiliary sources of supervision and multi-dataset training, for robust prediction of 3D hand poses on egocentric images in the wild. Experiments on both lab datasets and in-the-wild settings show the effectiveness of WildHands. As future direction, WildHands could be used to scale up learning robot policies from human interactions.

**Acknowledgements:** We thank Arjun Gupta, Shaowei Liu, Anand Bhattad & Kashyap Chitta for feedback on the draft, and David Forsyth for useful discussion. This material is based upon work supported by NSF (IIS2007035), NASA (80NSSC21K1030), DARPA (Machine Common Sense program), Amazon Research Award, NVIDIA Academic Hardware Grant, and the NCSA Delta System (supported by NSF OCI 2005572 and the State of Illinois).

## References

- [1] Shikhar Bahl, Abhinav Gupta, and Deepak Pathak. Human-to-robot imitation in the wild. In *RSS*, 2022. 1
- [2] Luca Ballan, Aparna Taneja, Jürgen Gall, Luc Van Gool, and Marc Pollefeys. Motion capture of hands in action using discriminative salient points. In *ECCV*, 2012. 2
- [3] Aude Billard, Sylvain Calinon, and Florent Guenter. Discriminative and adaptive imitation in uni-manual and bi-manual tasks. *Robotics Auton. Syst.*, 54(5):370–384, 2006. 1
- [4] Garrick Brazil, Abhinav Kumar, Julian Straub, Nikhila Ravi, Justin Johnson, and Georgia Gkioxari. Omni3d: A large benchmark and model for 3d object detection in the wild. In *CVPR*, pages 13154–13164, 2023. 8
- [5] Zhe Cao, Ilija Radosavovic, Angjoo Kanazawa, and Jitendra Malik. Reconstructing hand-object interactions in the wild. In *ICCV*, 2021. 2, 5, 6
- [6] Matthew Chang, Aditya Prakash, and Saurabh Gupta. Look ma, no hands! agent-environment factorization of egocentric videos. In *NeurIPS*, 2023. 1
- [7] Yu-Wei Chao, Wei Yang, Yu Xiang, Pavlo Molchanov, Ankur Handa, Jonathan Tremblay, Yashraj S. Narang, Karl Van Wyk, Umar Iqbal, Stan Birchfield, Jan Kautz, and Dieter Fox. Dexycb: A benchmark for capturing hand grasping of objects. In *CVPR*, 2021. 2, 6
- [8] Tianyi Cheng, Dandan Shan, Ayda Sultan Hassen, Richard Ely Locke Higgins, and David Fouhey. Towards a richer 2d understanding of hands at scale. In *NeurIPS*, 2023. 1, 2, 5, 6
- [9] Dima Damen, Hazel Doughty, Giovanni Maria Farinella, Sanja Fidler, Antonino Furnari, Evangelos Kazakos, Davide Moltisanti, Jonathan Munro, Toby Perrett, Will Price, et al. Scaling egocentric vision: The epic-kitchens dataset. In *ECCV*, 2018. 1, 2
- [10] Dima Damen, Hazel Doughty, Giovanni Maria Farinella, Sanja Fidler, Antonino Furnari, Evangelos Kazakos, Davide Moltisanti, Jonathan Munro, Toby Perrett, Will Price, and Michael Wray. The epic-kitchens dataset: Collection, challenges and baselines. *TPAMI*, 2020. 5
- [11] Ahmad Darkhalil, Dandan Shan, Bin Zhu, Jian Ma, Amlan Kar, Richard Higgins, Sanja Fidler, David Fouhey, and Dima Damen. Epic-kitchens visor benchmark: Video segmentations and object relations. In *NeurIPS Track on Datasets and Benchmarks*, 2022. 1, 2, 5
- [12] Jose M Facil, Benjamin Ummenhofer, Huizhong Zhou, Luis Montesano, Thomas Brox, and Javier Civera. Cam-convs: Camera-aware multi-scale convolutions for single-view depth. In *CVPR*, pages 11826–11835, 2019. 3
- [13] Zicong Fan, Adrian Spurr, Muhammed Kocabas, Siyu Tang, Michael J. Black, and Otmar Hilliges. Learning to disambiguate strongly interacting hands via probabilistic per-pixel part segmentation. In *3DV*, 2021. 6
- [14] Zicong Fan, Omid Taheri, Dimitrios Tzionas, Muhammed Kocabas, Manuel Kaufmann, Michael J. Black, and Otmar Hilliges. ARCTIC: A dataset for dexterous bimanual hand-object manipulation. In *CVPR*, 2023. 1, 2, 3, 4, 5, 6, 7
- [15] William T Freeman and Michal Roth. Orientation histograms for hand gesture recognition. In *International workshop on automatic face and gesture recognition*, pages 296–301. Cite-seer, 1995. 2
- [16] Guillermo Garcia-Hernando, Shanxin Yuan, Seungryul Baek, and Tae-Kyun Kim. First-person hand action benchmark with RGB-D videos and 3d hand pose annotations. In *CVPR*, 2018. 1, 2
- [17] Guillermo Garcia-Hernando, Shanxin Yuan, Seungryul Baek, and Tae-Kyun Kim. First-person hand action benchmark with rgb-d videos and 3d hand pose annotations. In *CVPR*, 2018. 2
- [18] Mohit Goyal, Sahil Modi, Rishabh Goyal, and Saurabh Gupta. Human hands as probes for interactive object understanding. In *CVPR*, 2022. 1
- [19] Kristen Grauman, Andrew Westbury, Eugene Byrne, Zachary Chavis, Antonino Furnari, Rohit Girdhar, Jackson Hamburger, Hao Jiang, Miao Liu, Xingyu Liu, et al. Ego4d: Around the world in 3,000 hours of egocentric video. In *CVPR*, 2022. 2
- [20] Vitor Guizilini, Igor Vasiljevic, Jiading Fang, Rare Ambru, Greg Shakhnarovich, Matthew R Walter, and Adrien Gaidon. Depth field networks for generalizable multi-view scene representation. In *ECCV*, 2022. 3
- [21] Vitor Guizilini, Igor Vasiljevic, Dian Chen, Rareş Ambruş, and Adrien Gaidon. Towards zero-shot scale-aware monocular depth estimation. In *ICCV*, 2023. 3
- [22] Shreyas Hampali, Mahdi Rad, Markus Oberweger, and Vincent Lepetit. Honnotate: A method for 3d annotation of hand and object poses. In *CVPR*, 2020. 2, 6
- [23] Shreyas Hampali, Sayan Deb Sarkar, Mahdi Rad, and Vincent Lepetit. Keypoint transformer: Solving joint identification in challenging hands and object interactions for accurate 3d pose estimation. In *CVPR*, 2022. 2, 6
- [24] Shangchen Han, Beibei Liu, Randi Cabezas, Christopher D. Twigg, Peizhao Zhang, Jeff Petkau, Tsz-Ho Yu, Chun-Jung Tai, Muzaffer Akbay, Zheng Wang, Asaf Nitzan, Gang Dong, Yuting Ye, Lingling Tao, Chengde Wan, and Robert Wang. Megatrack: monochrome egocentric articulated hand-tracking for virtual reality. *ACM Transactions on Graphics (TOG)*, 2020. 1
- [25] Shangchen Han, Po-Chen Wu, Yubo Zhang, Beibei Liu, Linguang Zhang, Zheng Wang, Weiguang Si, Peizhao Zhang, Yujun Cai, Tomas Hodan, Randi Cabezas, Luan Tran, Muzaffer Akbay, Tsz-Ho Yu, Cem Keskin, and Robert Wang. Umetrack: Unified multi-view end-to-end hand tracking for VR. In *SIGGRAPH*, 2022. 1
- [26] Richard Hartley and Andrew Zisserman. *Multiple view geometry in computer vision*. Cambridge university press, 2003. 3
- [27] Yana Hasson, Gül Varol, Dimitris Tzionas, Igor Kalevtykh, Michael J. Black, Ivan Laptev, and Cordelia Schmid. Learning joint reconstruction of hands and manipulated objects. In *CVPR*, 2019. 2, 5
- [28] Yana Hasson, Bugra Tekin, Federica Bogo, Ivan Laptev, Marc Pollefeys, and Cordelia Schmid. Leveraging photometric consistency over time for sparsely supervised hand-object reconstruction. *CVPR*, 2020. 2, 5, 6
- [29] Kaiming He, Xiangyu Zhang, Shaoqing Ren, and Jian Sun. Deep residual learning for image recognition. In *CVPR*, 2016. 4, 6

- [30] Tony Heap and David Hogg. Towards 3d hand tracking using a deformable model. In *Proceedings of the Second International Conference on Automatic Face and Gesture Recognition*, pages 140–145. Ieee, 1996. 2
- [31] Anthony Hu, Zak Murez, Nikhil Mohan, Sofia Dudas, Jeffrey Hawke, Vijay Badrinarayanan, Roberto Cipolla, and Alex Kendall. FIERY: future instance prediction in bird’s-eye view from surround monocular cameras. In *ICCV*, 2021. 8
- [32] Zhe Huang, Ye-Ji Mun, Xiang Li, Yiqing Xie, Ninghan Zhong, Weihang Liang, Junyi Geng, Tan Chen, and Katherine Rose Driggs-Campbell. Hierarchical intention tracking for robust human-robot collaboration in industrial assembly tasks. In *ICRA*, 2023. 1
- [33] Maksym Ivashchkin, Oscar Mendez, and Richard Bowden. Denoising diffusion for 3d hand pose estimation from images. *arXiv*, 2308.09523, 2023. 2
- [34] Changlong Jiang, Yang Xiao, Cunlin Wu, Mingyang Zhang, Jinghong Zheng, Zhiguo Cao, and Joey Tianyi Zhou. A2j-transformer: Anchor-to-joint transformer network for 3d interacting hand pose estimation from a single RGB image. In *CVPR*, 2023.
- [35] Zheheng Jiang, Hossein Rahmani, Sue Black, and Bryan M. Williams. A probabilistic attention model with occlusion-aware texture regression for 3d hand reconstruction from a single RGB image. In *CVPR*, 2023. 2
- [36] Angjoo Kanazawa, Michael J. Black, David W. Jacobs, and Jitendra Malik. End-to-end recovery of human shape and pose. In *CVPR*, 2018. 2
- [37] Angjoo Kanazawa, Shubham Tulsiani, Alexei A Efros, and Jitendra Malik. Learning category-specific mesh reconstruction from image collections. In *ECCV*, 2018. 2, 4, 6
- [38] Korrawe Karunratanakul, Jinlong Yang, Yan Zhang, Michael J Black, Krikamol Muandet, and Siyu Tang. Grasping field: Learning implicit representations for human grasps. In *3DV*, 2020. 2
- [39] Hiroharu Kato, Yoshitaka Ushiku, and Tatsuya Harada. Neural 3d mesh renderer. In *CVPR*, 2018. 2
- [40] Alex Kendall, Yarin Gal, and Roberto Cipolla. Multi-task learning using uncertainty to weigh losses for scene geometry and semantics. In *CVPR*, 2018. 8
- [41] Taein Kwon, Bugra Tekin, Jan Stühmer, Federica Bogo, and Marc Pollefeys. H2o: Two hands manipulating objects for first person interaction recognition. In *ICCV*, 2021. 2
- [42] Vincent Lepetit, Francesc Moreno-Noguer, and Pascal Fua. EPnP: An Accurate O(n) Solution to the PnP Problem. *IJCV*, 2009. 4
- [43] Fanqing Lin and Tony R. Martinez. Ego2handspose: A dataset for egocentric two-hand 3d global pose estimation. *arXiv*, 2206.04927, 2022. 2
- [44] Shichen Liu, Weikai Chen, Tianye Li, and Hao Li. Soft rasterizer: A differentiable renderer for image-based 3d reasoning. In *ICCV*, 2019. 2
- [45] Shichen Liu, Tianye Li, Weikai Chen, and Hao Li. A general differentiable mesh renderer for image-based 3d reasoning. *TPAMI*, 2020. 2, 5
- [46] Yunze Liu, Yun Liu, Che Jiang, Kangbo Lyu, Weikang Wan, Hao Shen, Boqiang Liang, Zhoujie Fu, He Wang, and Li Yi. HOI4D: A 4d egocentric dataset for category-level human-object interaction. In *CVPR*, 2022. 2, 6
- [47] Priyanka Mandikal and Kristen Grauman. Dexvip: Learning dexterous grasping with human hand pose priors from video. In *CoRL*, 2021. 1
- [48] Ben Mildenhall, Pratul P. Srinivasan, Matthew Tancik, Jonathan T. Barron, Ravi Ramamoorthi, and Ren Ng. Nerf: Representing scenes as neural radiance fields for view synthesis. In *ECCV*, 2020. 4
- [49] Takeru Miyato, Bernhard Jaeger, Max Welling, and Andreas Geiger. GTA: A geometry-aware attention mechanism for multi-view transformers. *arXiv*, 2023. 3
- [50] Gyeongsik Moon, Shoou-I Yu, He Wen, Takaaki Shiratori, and Kyoung Mu Lee. Interhand2.6m: A dataset and baseline for 3d interacting hand pose estimation from a single RGB image. In *ECCV*, 2020. 2, 6
- [51] Takehiko Ohkawa, Kun He, Fadime Sener, Tomas Hodan, Luan Tran, and Cem Keskin. Assemblyhands: Towards egocentric activity understanding via 3d hand pose estimation. In *CVPR*, pages 12999–13008, 2023. 1, 2, 5
- [52] Austin Patel, Andrew Wang, Ilija Radosavovic, and Jitendra Malik. Learning to imitate object interactions from internet videos. *arXiv preprint arXiv:2211.13225*, 2022. 1
- [53] Rolandos Alexandros Potamias, Stylianos Ploumpis, Stylianos Moschoglou, Vasileios Triantafyllou, and Stefanos Zafeiriou. Handy: Towards a high fidelity 3d hand shape and appearance model. In *CVPR*, pages 4670–4680, 2023. 2
- [54] Aditya Prakash, Arjun Gupta, and Saurabh Gupta. Mitigating perspective distortion-induced shape ambiguity in image crops. *arXiv*, 2023. 1, 3, 4, 5
- [55] Yuzhe Qin, Yueh-Hua Wu, Shaowei Liu, Hanwen Jiang, Ruihan Yang, Yang Fu, and Xiaolong Wang. Dexmv: Imitation learning for dexterous manipulation from human videos. In *ECCV*, 2022. 1
- [56] René Ranftl, Katrin Lasinger, David Hafner, Konrad Schindler, and Vladlen Koltun. Towards robust monocular depth estimation: Mixing datasets for zero-shot cross-dataset transfer. *TPAMI*, 44(3), 2022. 1
- [57] Nikhila Ravi, Jeremy Reizenstein, David Novotny, Taylor Gordon, Wan-Yen Lo, Justin Johnson, and Georgia Gkioxari. Accelerating 3d deep learning with pytorch3d. *arXiv:2007.08501*, 2020. 5
- [58] James M Rehg and Takeo Kanade. Visual tracking of high dof articulated structures: an application to human hand tracking. In *ECCV*, 1994. 2
- [59] Grégory Rogez, Maryam Khademi, JS Supančič III, Jose Maria Martinez Montiel, and Deva Ramanan. 3d hand pose detection in egocentric rgb-d images. In *ECCV*, 2014. 2
- [60] Javier Romero, Dimitrios Tzionas, and Michael J Black. Embodied hands: Modeling and capturing hands and bodies together. *ACM Trans. Gr.*, 2017. 2, 4, 5, 6
- [61] Yu Rong, Takaaki Shiratori, and Hanbyul Joo. Frankmocap: Fast monocular 3D hand and body motion capture by regression and integration. *ICCV Workshops*, 2021. 1, 2, 4, 6, 8
- [62] Fadime Sener, Dibyadip Chatterjee, Daniel Shelepov, Kun He, Dipika Singhania, Robert Wang, and Angela Yao. As-

- sembly101: A large-scale multi-view video dataset for understanding procedural activities. In *CVPR*, 2022. 1, 2
- [63] Dandan Shan, Jiaqi Geng, Michelle Shu, and David F Fouhey. Understanding human hands in contact at internet scale. In *CVPR*, 2020. 2
- [64] Toby Sharp, Cem Keskin, Duncan Robertson, Jonathan Taylor, Jamie Shotton, David Kim, Christoph Rhemann, Ido Leichter, Alon Vinnikov, Yichen Wei, et al. Accurate, robust, and flexible real-time hand tracking. In *Proceedings of the 33rd annual ACM conference on human factors in computing systems*, pages 3633–3642, 2015. 2
- [65] Tomas Simon, Hanbyul Joo, Iain A. Matthews, and Yaser Sheikh. Hand keypoint detection in single images using multiview bootstrapping. In *CVPR*, 2017. 2
- [66] Aravind Sivakumar, Kenneth Shaw, and Deepak Pathak. Robotic telekinesis: Learning a robotic hand imitator by watching humans on youtube. In *RSS*, 2022. 1
- [67] Srinath Sridhar, Antti Oulasvirta, and Christian Theobalt. Interactive markerless articulated hand motion tracking using RGB and depth data. In *ICCV*, 2013. 2
- [68] Srinath Sridhar, Franziska Mueller, Michael Zollhöfer, Dan Casas, Antti Oulasvirta, and Christian Theobalt. Real-time joint tracking of a hand manipulating an object from rgb-d input. In *ECCV*, 2016. 2
- [69] Xiao Sun, Yichen Wei, Shuang Liang, Xiaoou Tang, and Jian Sun. Cascaded hand pose regression. In *CVPR*, 2015. 2
- [70] Omid Taheri, Nima Ghorbani, Michael J Black, and Dimitrios Tzionas. GRAB: A dataset of whole-body human grasping of objects. In *ECCV*, 2020. 2, 6
- [71] Jonathan Tompson, Murphy Stein, Yann Lecun, and Ken Perlin. Real-time continuous pose recovery of human hands using convolutional networks. *ACM Transactions on Graphics (ToG)*, 33(5):1–10, 2014. 2
- [72] Shubham Tulsiani, Tinghui Zhou, Alexei A Efros, and Jitendra Malik. Multi-view supervision for single-view reconstruction via differentiable ray consistency. In *CVPR*, pages 2626–2634, 2017. 2
- [73] Dimitrios Tzionas and Juergen Gall. 3d object reconstruction from hand-object interactions. In *ICCV*, 2015. 2
- [74] Chengde Wan, Angela Yao, and Luc Van Gool. Hand pose estimation from local surface normals. In *ECCV*, 2016. 2
- [75] Lixin Yang, Kailin Li, Xinyu Zhan, Fei Wu, Anran Xu, Liu Liu, and Cewu Lu. Oakink: A large-scale knowledge repository for understanding hand-object interaction. In *CVPR*, 2022. 2
- [76] Yufei Ye, Abhinav Gupta, and Shubham Tulsiani. What’s in your hands? 3D reconstruction of generic objects in hands. In *CVPR*, 2022. 2, 6
- [77] Wang Yifan, Carl Doersch, Relja Arandjelović, Joao Carreira, and Andrew Zisserman. Input-level inductive biases for 3d reconstruction. In *CVPR*, 2022. 3
- [78] Xiong Zhang, Qiang Li, Hong Mo, Wenbo Zhang, and Wen Zheng. End-to-end hand mesh recovery from a monocular rgb image. In *ICCV*, 2019. 2
- [79] Christian Zimmermann and Thomas Brox. Learning to estimate 3d hand pose from single rgb images. In *ICCV*, 2017. 2
- [80] Christian Zimmermann, Duygu Ceylan, Jimei Yang, Bryan C. Russell, Max J. Argus, and Thomas Brox. Freihand: A dataset for markerless capture of hand pose and shape from single RGB images. In *ICCV*, 2019. 2